Optogenetic control of gut bacterial metabolism

Lucas A. Hartsough[1], Matthew V. Kotlajich[1], Bing Han[3,7], Chih-Chun J. Lin[3,4], Lauren Gambill[2], Meng C. Wang*[3,4,5], Jeffrey J. Tabor*[,1,2,6]

[1]Department of Bioengineering, [2]Systems, Synthetic, and Physical Biology Program, Rice University, Houston, TX; [3]Huffington Center on Aging, [4]Department of Molecular & Human Genetics, Baylor College of Medicine, Houston, TX; [5]Howard Hughes Medical Institute; [6]Department of Biosciences, Rice University; [7]Current Address: Children's Hospital & Institutes of Biomedical Sciences, Fudan University, Shanghai, China, 201102

*corresponding authors: wmeng@bcm.edu, jeff.tabor@rice.edu

Abstract

Gut bacteria produce a wide range of metabolites that impact host biology. However, *in situ* studies of microbe-host interactions are challenging due to the poor accessibility of the gut environment. Here, we develop a method wherein light is used to remotely control *E. coli* gene expression in the *C. elegans* gastrointestinal tract. We go on to engineer an *E. coli* strain from which secretion of the longevity-enhancing exopolysaccharide colanic acid (CA) is regulated by light. We then combine this strain with our optogenetic method to discover that CA produced by gut bacteria protects intestinal mitochondria from stress-induced hyper-fragmentation. Finally, we exploit the quantitative control of CA secretion afforded by light to reveal that CA extends worm lifespan in a dose-dependent manner. Optogenetic control of gut bacterial metabolism will enable new mechanistic studies of how the microbiome impacts health and disease.

Most microbiome studies identify correlations between bacterial and host biology. In particular, metagenomic DNA sequencing is often used to associate the presence or abundance of specific bacteria to a host physiological or diseased state[1–5]. Transcriptomic or metabolomic analyses are increasingly being included to shed light on the bacterial pathways responsible for host interactions[6,7] However, the observational nature of these approaches combined with the complexity and heterogeneity[8,9] of the gut environment make causality difficult to establish.

An ideal approach for studying microbiome-host interactions would be to directly manipulate gut bacterial gene expression and metabolism *in situ*. In several recent studies, researchers have administered small molecule inducers in drinking water to modulate gene expression from gut bacteria in mice[10–12]. Though useful, such chemical effectors are subject to slow and poorly-controlled transport, absorption, and degradation processes that ultimately limit their precision in the gastrointestinal (GI) tract.

Optogenetics combines light and genetically-engineered photoreceptors to achieve unrivaled control of biological processes[13]. Previously, we repurposed the green light-activated/red light de-activated two-component system (TCS) CcaSR to control *E. coli* gene expression with light[14,15]. Here, the sensor histidine kinase CcaS binds the co-produced chromophore phycocyanobilin (PCB) and adopts an inactive ground state. Green light exposure switches CcaS to an active state, wherein it phosphorylates the response regulator CcaR. Phosphorylated CcaR then activates transcription from the $P_{cpcG2\text{-}172}$ output promoter. Red light reverts active CcaS to the inactive form, de-activating $P_{cpcG2\text{-}172}$. We and others have used CcaSR to achieve precise quantitative, temporal, and spatial control of *E. coli* gene expression *in vitro*[14–19].

The roundworm *C. elegans* has a short lifespan and well-defined microbiota, making it a tractable model organism for investigating how gut bacteria impact aging[20], among other

biological processes. Furthermore, *C. elegans* can be reared on a single *E. coli* strain that populates the GI tract and constitutes the entire microbiome, facilitating mechanistic studies of bacterial-host interactions[21,22]. In addition, the body of this worm is entirely transparent, which enables simple optical manipulations.

In previous work, we combined *E. coli* gene knockouts with *C. elegans* lifespan measurements to discover bacterial genes whose inactivation prolongs host lifespan[22]. Several of the *E. coli* gene deletions result in overproduction of the secreted exopolysaccharide colanic acid (CA). We demonstrated that purified CA is sufficient to extend worm lifespan by increasing mitochondrial fragmentation in intestinal cells[22]. However, it remains unclear whether inducing CA secretion from gut bacteria *in situ* is sufficient to modulate mitochondrial dynamics, and whether CA enhances longevity in a dose-dependent manner. Here, we hypothesized that a method enabling optogenetic control of CA production from gut bacteria would enable us to address these questions.

Results

Optogenetic control of gut bacterial gene expression

To demonstrate optogenetic control over gut bacterial gene expression, we engineered *E. coli* strain LH01, wherein CcaSR controls expression of superfolder green fluorescent protein (*sfgfp*)[23] and *mcherry*[24] is expressed constitutively to facilitate identification of the bacteria (**Fig. 1a**, **Supplementary Fig. 1, Supplementary Tables 1-3**). Then, we reared two groups of *C. elegans* from the larval to the adult stage on plates of LH01 under red or green light, respectively (**Fig. 1b**). Next, we washed away external bacteria, applied the paralyzing agent levamisole to prevent expulsion of gut contents, and transferred the worms to agar pads. Finally, we switched

the light color from red to green, or green to red, and used epi-fluorescence microscopy to image the resulting changes in fluorescence in the gut lumen over time (**Fig. 1c**). In the red-to-green (step ON) experiment, we observe that sfGFP fluorescence in the worm gut lumen starts low, begins to increase within 2 hours, and reaches a saturated high level at 6 hours (**Fig. 1d**). In contrast, in the green-to-red (step OFF) experiment, sfGFP fluorescence begins high, and decreases exponentially between hours 1-7 (**Fig. 1d**). These data demonstrate reversible control of bacterial gene expression in the gut of a live host and are consistent with exponential bacterial growth. As expected, the bacterial light response is abolished when worms are reared on control *E. coli* lacking the PCB biosynthetic operon (ΔPCB) (**Fig. 1d**).

Next, we used flow cytometry to examine how engineered gut bacteria respond to light with single-cell resolution. Specifically, we reared worms in red and green light as before, but then washed, paralyzed, and placed them into microtubes prior to light switching (**Fig. 1b**). At several time points over the course of 8 hours, we homogenized the animals, harvested the gut contents, and measured fluorescence via cytometry. This experiment revealed that our bacteria remain intact (**Supplementary Fig. 2**) and respond to light in a unimodal fashion (**Fig. 1e-g**) in the gut. Furthermore, the gene expression response dynamics and ΔPCB controls recapitulate our microscopy results (**Supplementary Fig. 3)**. We confirmed that residual bacteria on the exterior of worms do not contribute to our flow cytometry measurements (**Supplementary Fig. 4**). These experiments demonstrate that we can use optogenetics to control *E. coli* gene expression in the *C. elegans* gut.

Optogenetic control of CA secretion

To place CA secretion under optogenetic control, we expressed *rcsA*, which activates transcription of the CA biosynthetic operon[25], under control of CcaSR in a Δ*rcsA* strain background (**Fig. 2a, Supplementary Tables 1-3)**. Then, we grew this strain (named MVK29) in batch culture under red or green light and quantified supernatant CA levels. In red light, MVK29 secretes CA to concentrations below the limit of detection of the assay (~2 μg fucose mL^{-1} OD_{600}^{-1}), similar to the Δ*rcsA* control strain (**Fig. 2b**). As expected, green light induces MVK29 to secrete high levels of CA (54.9 ± 1.5 μg fucose mL^{-1} OD_{600}^{-1}; **Fig. 2b**). Deletion of the PCB biosynthetic operon results in light-independent intermediate CA levels (~13 μg fucose mL^{-1} OD_{600}^{-1}) consistent with our previous characterization of CcaSR[23]. Mutation of the CcaS catalytic histidine to a non-functional alanine (H534A), and the CcaR phosphorylation site to a non-functional asparagine (D51N) also abolish detectable CA production (**Fig. 2b**), consistent with low phospho-signaling. Finally, CA levels increase sigmoidally with green light intensity, similar to the response of CcaSR itself (**Fig. 2c**)[15]. We conclude that we can use CcaSR to control the extent of CA secretion from *E. coli*.

<u>*In situ* CA secretion protects against mitochondrial hyper-fragmentation</u>

To analyze the effects of light-induced CA secretion on *C. elegans*, we first reared worms expressing mitochondrially-localized GFP (**Supplementary Table 3**) on MVK29 red light as before. We then continued this red light exposure for one group, and switched a second to green, for an additional 6 hours, and immediately imaged intestinal cell mitochondrial morphology using confocal microscopy (**Fig. 3b**). We found that mitochondrial fragmentation increases in worms exposed to the bacteria with light-induced CA secretion (**Fig. 3c**). This result recapitulates the

phenotype observed when worms are supplemented with purified CA[22]. Thus, we can use bacterial optogenetics to modulate *C. elegans* mitochondrial dynamics.

Light-regulated CA secretion extends worm lifespan

Next, we examined the effect of light-induced CA from bacteria residing within the host gut. To this end, we paralyzed the worms, split them into two groups, and treated one with red and the second with green for 6 additional hours (**Fig. 3a**). We then analyzed the morphology of the intestinal cell mitochondrial network as before. First, we found that levamisole treatment results in mitochondrial hyper-fragmentation (**Fig. 3d**). This stress-induced effect resembles mitochondrial decay related to aging and age-related neurodegenerative diseases [26–28]. Additionally, we found that green light treatment of paralyzed worms bearing MVK29 in the GI tract counteracts this hyper-fragmentation (**Fig. 3d**). This protective effect did not occur when we fed paralyzed worms ΔPCB, CcaS(H534A), CcaR(D51N) or *ΔrcsA* control strains (**Fig. 3d**). These results show that we can use light to induce CA secretion from gut-borne *E. coli*, and that CA secreted by gut bacteria protects *C. elegans* intestinal cell mitochondria from stress-induced fragmentation.

Finally, we investigated whether light-induced CA secretion extends *C. elegans* lifespan. Beginning at the day-1 adult stage, we exposed worms feeding on MVK29 to red, or green light intensities resulting in intermediate or saturating CA secretion, and measured the resulting worm lifespans. Indeed, we found that *C. elegans* lifespan increases with green-light intensity, and the extent of lifespan extension is much stronger than that caused by CA supplementation [22] (**Fig. 4a**). This experiment reveals that the pro-longevity effect of CA is dose-dependent. As a control, we repeated the experiment with *E. coli* lacking the *lon* protease gene (Δ*lon*), which constitutively

secretes high levels of CA. As expected, *C. elegans* fed the Δ*lon* strain exhibit extended lifespan regardless of light treatment (**Fig. 4b**). The extent of lifespan extension is similar to the MVK29 intermediate green light condition, but less than the MVK29 saturating green light condition (**Fig. 4a, b**), suggesting MVK29 secretes higher levels of CA than Δ*lon* in saturating green light. Lifespan is also light-independent when worms are fed the Δ*rcsA* strain, and these worms exhibit lifespans comparable to those fed MVK29 under red light (**Fig. 4a, c**). These results suggest that optogenetic control is sufficient to induce bacterial production of pro-longevity compounds and improve host health, and can exert stronger beneficial effects than administration of a bacterial mutant or supplementing of purified compounds. Importantly, unlike introducing a bacterial mutant, optogenetic control of bacterial metabolism can modulate a host-level phenotype in a quantitative manner.

Discussion

Our method has broad applications for studying microbe-host interactions *in situ*. For example, we have identified about two dozen additional *E. coli* genes that are unrelated to CA biosynthesis and that enhance worm longevity when knocked out[22], though the mechanisms by which they act remain largely unclear. By using light to induce their expression in the gut, and measuring acute host responses such as changes in mitochondrial dynamics, the role of these genes in gut microbe-host interactions could be further explored. In another example, the quorum-sensing peptide CSF and nitric oxide, both of which are produced by *Bacillus subtilis* during biofilm formation, have been found to extend worm lifespan through downregulation of the insulin-like signaling pathway[29]. We have recently ported CcaSR into *B. subtilis* and demonstrated that it enables rapid and precise control of gene expression dynamics[30]. The method we report here

should enable *in situ* studies of how gene expression and metabolite production from this important Gram-positive model bacterium impact the worm as well.

Multiple photoreceptors could also be combined to study more complex microbe-host interaction pathways. Specifically, we and others have co-expressed CcaSR with independently-controllable blue/dark and red/far-red reversible light sensors in order to achieve simultaneous and independent control of the expression of up to three genes in the same bacterial cell[14,17,31]. Such optogenetic multiplexing could be performed *in situ* and used to study potential synergistic, antagonistic, or other higher-order effects of multiple bacterial genes or pathways. A large number of eukaryotic photoreceptors have also been developed, enabling optical control of many cell- and neurobiological processes[32–35]. Bacterial and eukaryotic photoreceptors could be combined to enable simultaneous optical manipulation of bacterial and host pathways in order to interrogate whether or how they interact. Optogenetics could also be used to manipulate bacterial and/or host pathways at specific locations within the gut to examine location- or tissue-dependent phenomena.

Finally, our method could be extended to other bacteria or hosts. In particular, it should be possible to port CcaSR or other bacterial photoreceptors into native *C. elegans* symbionts[36] or pathogens[37]. Because these strains stably colonize the host, the use of these bacteria could eliminate the need for paralysis, and facilitate longer-term experiments. It is likely that light can also be used to control gut bacterial gene expression in other model hosts such as flies, zebrafish, or mammals. Red-shifted wavelengths and corresponding optogenetic tools[38,39] may prove superior for less optically transparent or larger animals. Overall, by enabling precision control of bacterial gene expression and metabolism *in situ*, we believe that optogenetics will greatly improve our understanding of a wide range of microbe-host interactions.

Acknowledgements

The LED array used to illuminate *C. elegans* plates was designed by Brian Landry & Sebastián Castillo-Hair. The mounting hardware for the microscope LED array was designed by Ravi Sheth. We thank Ravi Sheth for discussions during early stages of the project. We thank Dr. Joel Moake for the use of his cytometer. This work was supported by the John S. Dunn Foundation (J.J.T. and M.C.W.) and US National Institutes of Health, 1R21NS099870-01 (J.J.T.), DP1DK113644 (M.C.W.), R01AT009050 (M.C.W.). LAH was supported by a NASA Office of the Chief Technologist Space Technology Research Fellowship (NSTRF NNX11AN39H).

Author Contributions

JJT and MW conceived of the study. LAH and MVK designed experiments. MVK and LAH constructed plasmids and strains. LAH, MVK, BH, CJL, LG, and MW performed experiments. CJL and LG scored single-blinded mitochondrial confocal micrographs. LAH, MVK, and MW analyzed and interpreted results. LAH, MW, and JJT wrote the manuscript.

Declaration of Interests

The authors declare no competing interests.

Figures and legends

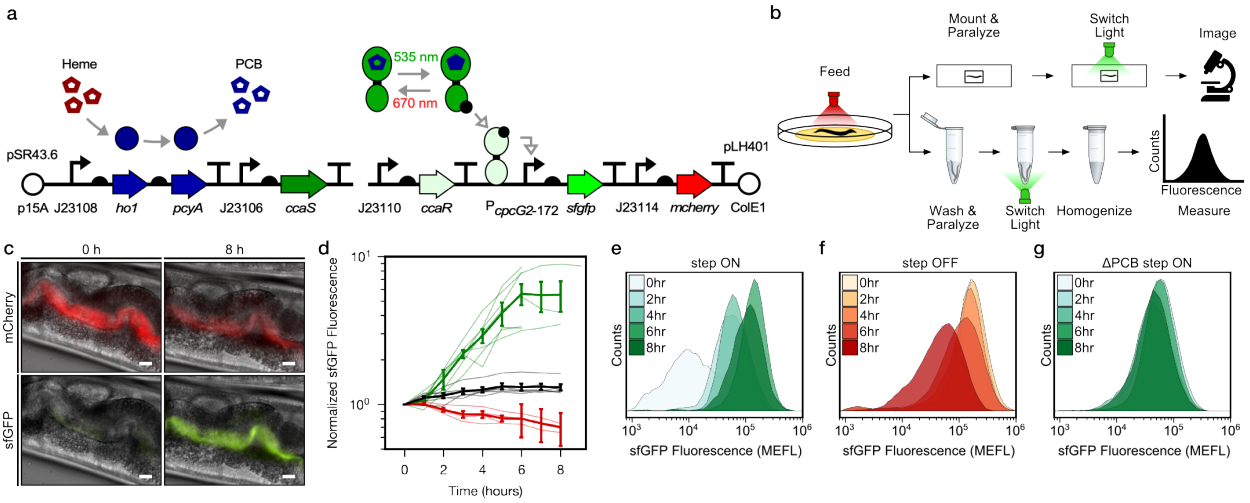

Figure 1. Optogenetic control of *C. elegans* gut bacterial gene expression. (a) Strain LH01. (b) Microscopy and cytometry workflows. (c) Fluorescence microscopy images 0 and 8 h after green light exposure in the step ON experiment. Scale bar: 10 μm. (d) Response dynamics in the step ON (green) and step OFF (red) microscopy experiments. Black: ΔPCB strain (step ON experiment). Individual- (light lines) and multi-worm average (dark lines) data are shown. n = 7, 4, 6 worms for green, red, black data sets (measured over 2, 3, 1 days, respectively). Error bars: SEM. (e-g) Flow cytometry histograms for response dynamics experiments. MEFL: molecules of equivalent fluorescein.

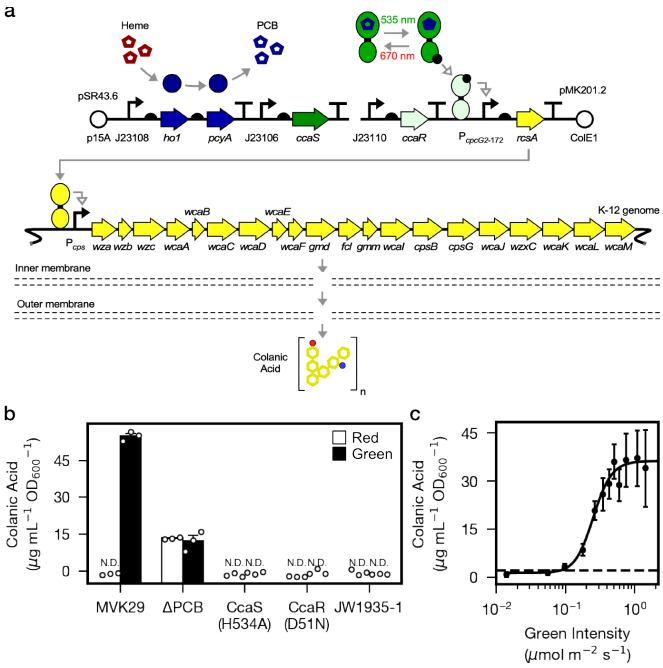

Figure 2. Optogenetic control of colanic acid biosynthesis. (a) Strain MVK29. (b) CA secretion levels for MVK29 and control strains exposed to red and green light. N.D.: below assay limit of detection. (c) Green light intensity versus CA secretion level for MVK29. Data points represent 3 biological replicates collected on a single day. Dashed line: limit of detection. Error bars indicate standard deviation of the three biological replicates.

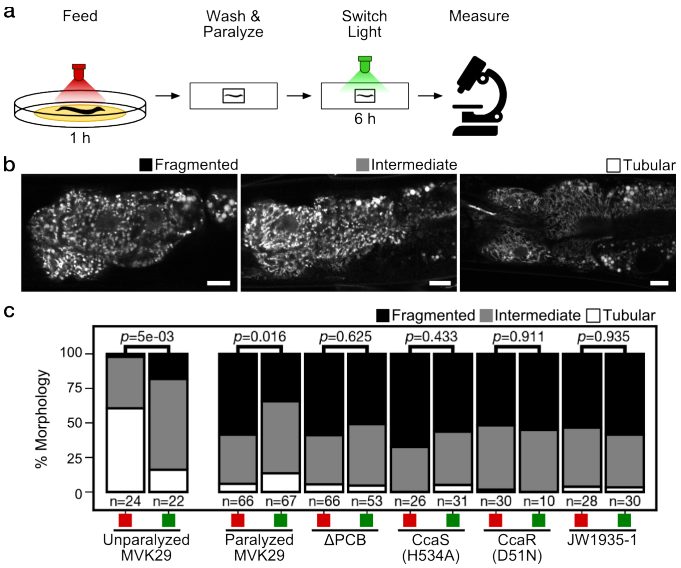

Figure 3. Light-regulated CA secretion modulates *C. elegans* mitochondrial dynamics. (a) Schematic of experiment for activating CA biosynthesis *in situ*. (b) Representative images of the mitochondrial network of anterior intestinal cells immediately distal to the pharynx are scored as fragmented, intermediate, or tubular, as previously [22]. Scale bars: 10 μm. (c) Mitochondrial fragmentation profiles of un-paralyzed worms fed MVK29 while exposed to red or green light for 6 h. (d) Fragmentation profiles for worms fed the indicated strain, then paralyzed for 6 h while exposed to red or green light. The number of worms included in each condition is indicated below each bar. The Chi-Squared Test of Homogeneity was used to calculate *p*-values between conditions.

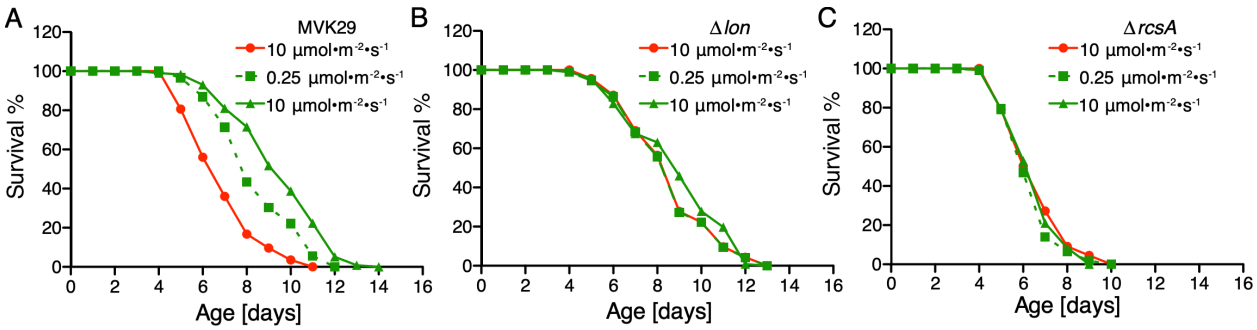

233

234 **Figure 4. Optogenetically-regulated CA biosynthesis extends worm lifespan.** (a) When
235 exposed to green light, worms grown on MVK29 live longer than those exposed to red light, and
236 the magnitude of lifespan extension is proportional to green light intensity ($p<0.0001$ green vs.
237 red, log-rank test). (b-c) The lifespans of worms grown on the Δ*lon* (b) or the Δ*rcsA* (c) controls
238 are not affected by light condition ($p>0.1$ green vs. red, log-rank test).

239

240

Methods

E. coli plasmids, strains, and media

Plasmids used in this study are described in **Supplementary Table 1**. Genbank accession numbers are given in **Supplementary Table 2**. All plasmids constructed in this study were assembled via Golden Gate cloning[40]. Primers were ordered from IDT (Coralville, IA). Assembled plasmids were transformed into *E. coli* NEB10β (New England Biolabs) for amplification and screening. All plasmid sequences were confirmed by Sanger sequencing (Genewiz; S. Plainfield, NJ). To construct pLH401 and pLH405, pSR58.6[15] was modified by inserting an *mCherry* expression cassette composed of a constitutive promoter (J23114; http://parts.igem.org/Promoters/Catalog/Anderson), RBS (BBa_B0034; http://parts.igem.org/Part:BBa_B0034), *mCherry*, and a synthetic transcriptional terminator (L3S1P52 [41]). To construct pLH405, pLH401 was further modified by exchanging the superfolder GFP gene (*sfgfp*) for *gfpmut3**. pMVK201.2 was built by modifying pSR58.6 to control expression of *rcsA*.

All *E. coli* strains are described in **Supplementary Table 3.** *ΔrcsA* (JW1935-1) was obtained from the Coli Genetic Stock Center. *Δlon* (JW0429-1) was obtained from the Keio *E. coli* knockout library[42], a gift from the Herman lab. All *E. coli* strains were maintained in LB media supplemented with appropriate antibiotics (chloramphenicol 34 μg/mL, spectinomycin 100 μg/mL, kanamycin 100 μg/mL) in a shaking incubator at 37°C and 250 rpm unless otherwise noted.

261

262 *C. elegans* strains and media

263 All *C. elegans* strains (**Supplementary Table 3**) were provided by the Caenorhabditis
264 Genetics Center (University of Minnesota), which is funded by the NIH office of Research
265 Infrastructure Programs (P40 OD010440). Worms were grown at 20°C on 1.7% NGM-agar plates
266 in 60 mm Petri dishes inoculated with a lawn of *E. coli* (CGSC str. BW28357), as described in the
267 CGC WormBook (wormbook.org), unless otherwise specified. The common strain *E. coli* OP50
268 was not used for worm feeding, as it produces CA during normal growth[22]. M9 buffer for *C.*
269 *elegans* (abbreviated M9Ce to distinguish from *E. coli* M9 media) was composed of 3 g KH_2PO_4,
270 6 g Na_2HPO_4, 5 g NaCl, 1 mL 1 M $MgSO_4$, H_2O to 1 L, and sterilized by autoclaving
271 (wormbook.org).

272

273 Optogenetic control of CA production

274 3 mL starter cultures of appropriate *E. coli* strains were inoculated from a -80°C freezer
275 and grown 12 h at 37°C. These starters were diluted to $OD_{600} = 1x10^{-2}$ in M9 minimal media (1x
276 M9 salts, 0.4% w/v glucose, 0.2% w/v casamino acids, 2 mM $MgSO_4$, 100 μM $CaCl_2$)
277 supplemented with appropriate antibiotics. The M9/cell mixtures were then distributed into 3 mL
278 aliquots in 15 mL clear polystyrene culture tubes and grown at 37°C in a shaking incubator at 250
279 rpm while illuminated with the appropriate light wavelength and intensity, using the Light Tube
280 Array (LTA) device[43]. After 22 h, cultures were removed and iced to halt growth and the OD_{600}
281 was measured. Culture samples were collected for CA quantification.

282

283 CA quantification

284 We adapted a previous CA quantification protocol[44,45] that takes advantage of the fact that
285 it is the only exopolysaccharide produced in our *E. coli* strains that incorporates fucose. In
286 particular, we quantified the amount of fucose in cell-derived exopolysaccharides (EPS), and used
287 that value as a proxy CA levels. First, EPS was liberated from cells by boiling 2 mL of culture for
288 15 min. in a 15 mL conical tube. The sample was then centrifuged in 1.5 mL Eppendorf tubes for
289 15 min. at 21,000 x g. Then, 0.7 mL of supernatant was dialyzed against water for at least 12 h
290 using Pur-A-Lyzer Midi 3500 dialysis mini-tubes (Sigma-Aldrich, PURD35100-1KT) to remove
291 monomeric fucose from the sample.

292 Fucose monomers were then liberated from the EPS polymers by hydrolyzing 0.2 mL of
293 dialyzed media with 0.9 mL of H_2SO_4 solution (6:1 v/v acid:water). This mixture was boiled in a
294 15 mL conical for 20 min and then cooled to room temperature. The absorbance at 396 nm and
295 427 nm was measured. Next, 25 μL of 1 M L-cysteine HCl was added and mixed thoroughly by
296 pipetting. The absorbance at 396 nm and 427 nm was measured again. Simultaneously, absorbance
297 measurements of L-fucose standards pre- and post-L-cysteine addition were also recorded.
298 Absorbance change, given by *D* in the formula below, were used to compare the L-fucose standard
299 samples to the dialyzed culture samples and estimate the L-fucose concentration in the dialyzed
300 product.

301 $$D = \left(\left(A_{post}^{396} - A_{pre}^{396}\right) - \left(A_{post}^{427} - A_{pre}^{427}\right)\right)$$

302

303 Preparation of NGM-agar plates for worm feeding

304 3 mL *E. coli* starter cultures were inoculated from -80°C freezer stocks and grown for 12
305 h at 37°C. These starters were then diluted to OD_{600} = 1 x 10^{-6} in M9 minimal media supplemented
306 with appropriate antibiotics. The M9/cell mixture was then distributed into 3mL aliquots in 15 mL
307 clear polystyrene culture tubes and grown at 37°C in a shaking incubator at 250 rpm while
308 illuminated with the appropriate light in the LTA. Once cultures reached OD_{600} = 0.1-0.4, tubes
309 were iced for 10 min and subsequently concentrated to OD_{600} ~ 20 by centrifugation (4°C, 4000
310 rpm, 10 min) and resuspension in fresh M9 media. 400-600 μL of dense bacterial culture was then
311 applied to sterile NGM-agar plates and allowed to dry in a dark room, or a room with green
312 overhead safety lights if cultures were preconditioned in green light. Plates were wrapped in foil
313 and refrigerated at 4°C for no more than 5 days until needed.

314

315 Time-lapse microscopy

316 To obtain age-synchronized worm cultures, axenized *C. elegans* (strain *glo-1*) eggs were
317 isolated and allowed to arrest in L1 by starvation in M9 buffer (distinct from M9 media: 3 g
318 KH_2PO_4, 6 g Na_2HPO_4, 5 g NaCl, 1 mL 1M $MgSO_4$, and water to 1 L, sterilized by autoclaving at
319 121°C for 20 min) at room temperature for 12-18 h. 10-100 larvae were transferred to a previously
320 prepared NGM-agar plate containing a lawn of the appropriate bacterial strain. The plate was then
321 placed in a 20°C incubator and illuminated with appropriate optogenetic light provided by a single
322 LED positioned 1cm above the Petri dish. Adult worms were transferred to a fresh plate as
323 necessary to maintain only a single generation.

Individual worms aged 1-3 days were removed from the dish and prepared for time-lapse epifluorescence imaging. A 1.5% agar pad was prepared using M9 buffer as previously described[45], and punched into ½" circles with a hollow punch. A 4 µL droplet of 2 mM levamisole was deposited on a pad and 5 adult worms were transferred from the NGM plate to the droplet. An additional 4 µL of levamisole solution was added and the worms were gently washed to remove external bacteria. Worms were then transferred to a fresh pad with a 4 µL droplet of levamisole solution, which was allowed to dry, thereby co-localizing and aligning the worms on the pad. The pad was then inverted and placed into a 13 mm disposable microscopy petri dish with a #1.5 coverslip on the bottom (Cell E&G; Houston, TX). Another coverslip was placed on the top of the pad in the dish to curtail evaporation.

The dish was then placed on the stage of a Nikon Eclipse Ti-E inverted epifluorescence microscope (Nikon Instruments, Inc; Melville, NY). Complete paralysis was induced by incubating the dish at room temperature (~23°C) for 30 min. Meanwhile, worms were exposed to appropriate preconditioning light supplied by a circular array of 8 LEDs (4 x 660 nm, 4 x 525 nm) mounted to the microscope condenser ring, about 2 cm above the Petri dish. Light was then switched from the preconditioning to the experimental wavelength, and worms were imaged periodically using 10x, 40x, and 60x objectives. For each time point, the LEDs were turned off and images acquired in the brightfield (DIC) and fluorescent channels. Afterwards, the LEDs were turned on again to maintain optogenetic control.

Epifluorescence image analysis

All epifluorescence images were analyzed using the Nikon Elements software package (Nikon Instruments, Inc; Melville, NY). The mCherry signal was used as a marker for the gut

lumen, and only cells in this region were included in the analysis. Image ROIs were created by thresholding the sfGFP signal to identify the boundaries of cell populations. Out of focus regions were eliminated from analysis. The average sfGFP pixel intensity inside the ROIs was calculated and recorded for each time point.

Flow cytometry

1-3 day old *glo-1* worms were prepared for flow cytometry of the microbiome constituents by washing, using a protocol adapted from previous work[46]. Groups of 5 worms were washed 2x in a 5 µL droplet of lytic solution: *C. elegans* M9 buffer containing 2 mM levamisole, 1% Triton X-100, and 100 mg/mL ampicillin. The worms were then washed 2x in 5 µL droplets of M9 buffer containing 2 mM levamisole only. Finally, the worms were transferred to clear 0.5 mL Eppendorf tubes containing 50 µL of M9 buffer + 2 mM levamisole, ensuring that 5 worms were deposited in the liquid contained in each tube. Each tube was then exposed to light by placing it within one well of a 24-well plate (AWLS-303008, ArcticWhite LLC) atop a Light Plate Apparatus (LPA) containing green and red LEDs[47] for 8 h at room temperature. In separate control experiments, we demonstrated that any stray bacteria that may escape the worms over this period, or which were inadvertently added to the 50 µL of M9 buffer, are incapable of responding to optogenetic light (**Supplementary Fig. 4**).

At the conclusion of the experiment, tubes were removed from the plate and immediately chilled in an ice slurry for 10 min in the dark. Worms were homogenized using an anodized steel probe sterilized between samples via 70% ethanol treatment and flame before being cooled.

Next, we used our previous antibiotic-based fluorescent protein maturation protocol[16] to allow unfolded proteins to mature while preventing the production of new protein. In particular, 250 μL PBS containing 500 mg/mL Rifampicin was added to the 50 μL homogenized worm samples and transferred to cytometry tubes. These tubes were incubated in a 37°C water bath for precisely 1 h, then transferred back to an ice slurry.

These samples were measured on a BD FACScan flow cytometer. For gating, an FSC/SSC polygon gate was first created using non-fluorescent bacteria grown *in vitro* at 37°C (**Supplementary Fig. 2**). Events outside this region were excluded as non-bacterial material. To isolate the engineered gut bacteria, only events with a high mCherry signal (FL3 > 1200 a.u., FL3 gain: 999) were included (**Supplementary Fig. 2**). Samples were measured until 20,000 events were recorded or the sample was exhausted.

Flow cytometry data analysis

All flow cytometry data (FCS format) were analyzed using FlowCal[47] and Python 2.7. We wrote a standard cytometry analysis workflow that truncated the initial and final 10 events to prevent cross-sample contamination, removed events from saturated detector bins at the ends of the detection range, and added 2D density gate on SSC/FSC retaining the densest 75% of events (**Supplementary Fig. 2a**). GFPmut3* fluorescence units were converted into standardized units of molecules of equivalent fluorescein (MEFL) using a fluorescent bead standard (Rainbow calibration standard; cat. no. RCP-30-20A, Spherotech, Inc.) as described previously[47]. Finally, to eliminate events associated with *C. elegans* autofluorescence (**Supplementary Fig. 2b**), any events in the region FL1 $\leq$ 1200 MEFL were discarded.

390

391 Mitochondrial Fragmentation Assays

392 Synchronized L1 worms (strain *ges-1*) were applied to NGM agar plates containing
393 bacterial strain BW25113 and allowed to develop until adulthood. This parental bacterial strain is
394 used to allow all worms to develop at the same rate, avoiding any developmental/growth effects
395 the experimental strains may exert on the worms. All experimental bacterial strains were
396 preconditioned in red light with optogenetic light provided by a single LED positioned 1 cm above
397 the Petri dish.

398 After 3-5 days (between days 1-3 of adulthood), worms allocated for the experiment were
399 transferred to experimental strains for approximately 60-90 minutes to thoroughly inoculate the
400 GI tract. In the case of the unparalyzed worms, red or green light was then applied for an additional
401 6 hours. For the paralyzed worm experiments, 1.5% low-melt agar pads were prepared as described
402 above and placed on individual slides. About 15 adult worms were transferred from the
403 experimental strain Petri dish to an agar pad containing 10 µL of *C. elegans* M9 buffer + 2 mM
404 levamisole (M9Ce+Lev), where worms were gently washed before being transferred to a fresh pad
405 also containing 10 µL of M9Ce+Lev. The majority of M9Ce+Lev on the pad was allowed to
406 evaporate, which causes the worms to align longitudinally before a cover slip was applied. Slides
407 were then exposed to either red or green light by placing them under a single LED positioned 1
408 cm above the Petri dish for 6 h. Afterward, the anterior intestinal cells were imaged using confocal
409 microscopy (Olympus Fluoview 3000) in the brightfield and GFP channels.

410

411 Confocal Microscopy Image Analysis

412 All confocal images for an experiment were manually cropped to display only the anterior
413 intestinal cells of a single worm (in the GFP channel). These cropped images were then
414 anonymized, randomized and the mitochondrial networks of each were blindly classified by two
415 researchers independently as either tubular, fragmented, or intermediate. Tubular samples were
416 marked by a high degree of network connectivity throughout. Fragmented samples were composed
417 almost exclusively of isolated clusters of fluorescence with high circularity. Intermediate samples
418 contained regions of both types. Scores were then de-randomized and aggregated. For each
419 experimental strain, the red and green light conditions were compared for statistical significance
420 using the chi-squared test of homogeneity.

421

422 Lifespan experiments

423 3 mL starter cultures of Δ*lon*, Δ*rcsA* or MVK29 were inoculated from -80ºC freezer stocks
424 into LB supplemented with appropriate antibiotics and grown shaking for 12 h at 37 ºC at 250 rpm.
425 These cultures were diluted to OD_{600} = $1x10^{-6}$ in 27 mL M9 media supplemented with appropriate
426 antibiotics. 1.5 mL of each M9/cell mixture was added to each of 18 wells on three 24-well plates
427 and grown in 3 LPA devices under the appropriate light conditions at 37 ºC and 250 rpm. Once
428 cultures reached OD_{600} = 0.1-0.4, all tubes were iced for 10 min and subsequently concentrated 10
429 times by centrifugation (4ºC, 4000 rpm, 10 min). Approximately 50 µL of this dense bacterial
430 culture was then applied to sterile NGM-agar plates with no antibiotics and allowed to dry in a
431 dark room. The plates were then illuminated with the appropriate light wavelength and intensity
432 for 16 h at room temperature, and immediately used for lifespan assays.

During the longitudinal lifespan assay, exposure to white light is limited to the minimal level. To reach this goal, the *sqt-3(e2117)* temperature sensitive mutant (**Supplementary Table 3**) was used to perform longitudinal analyses at 25 ºC, which avoids time-consuming animal transfer without interrupting normal reproduction. *sqt-3(e2117)* is a collagen mutant of *C. elegans* that reproduces normally but is embryonically lethal at 26 ºC, and has been used previously in longitudinal studies[22,48]. Worms were age-synchronized by bleach-based egg isolation followed by starvation in M9 buffer at the L1 stage for 36 hours. Synchronized L1 worms were grown on BW25113 *E. coli* at 15 ºC until the L4 stage, when worms were transferred to 24-well plates (~15 worms/well) with Δ*lon*, Δ*rcsA* or MVK29 (**Supplementary Table 3**). The plates were placed in LPA. The LPA LEDs were programmed to illuminate wells with constant red (10 μmol/m²/s), low-intensity green (0.25 μmol/m²/s), or high-intensity green light (10 μmol/m²/s). The apparatus was then transferred to a 26 ºC incubator. The number of living worms remaining in each well was counted every day. Death was indicated by total cessation of movement in response to gentle mechanical stimulation. Statistical analyses were performed with SPSS (IBM Software) using Kaplan-Meier survival analysis and the log-rank test (**Supplementary Table 4**).

References

1. Zhernakova, A. *et al.* Population-based metagenomics analysis reveals markers for gut microbiome composition and diversity. *Science* **352**, 565–569 (2016).

2. Qin, J. *et al.* A metagenome-wide association study of gut microbiota in type 2 diabetes. *Nature* **490**, 55–60 (2012).

3. Kostic, A. D. *et al.* The dynamics of the human infant gut microbiome in development and in progression toward type 1 diabetes. *Cell Host Microbe* **17**, 260–73 (2015).

456 4. Graessler, J. *et al.* Metagenomic sequencing of the human gut microbiome before and after
457 bariatric surgery in obese patients with type 2 diabetes: correlation with inflammatory and
458 metabolic parameters. *Pharmacogenomics J* **13**, 514–522 (2012).

459 5. Bisanz, J. E., Upadhyay, V., Turnbaugh, J. A., Ly, K. & Turnbaugh, P. J. Meta-Analysis Reveals
460 Reproducible Gut Microbiome Alterations in Response to a High-Fat Diet. *Cell Host Microbe* **26**,
461 265-272.e4 (2019).

462 6. Turnbaugh, P. J. & Gordon, J. I. An Invitation to the Marriage of Metagenomics and
463 Metabolomics. *Cell* **134**, 708–713 (2008).

464 7. Aguiar-Pulido, V. *et al.* Metagenomics, Metatranscriptomics, and Metabolomics Approaches
465 for Microbiome Analysis. *Evol Bioinform Online* **12**, 5–16 (2016).

466 8. Sheth, R. U. *et al.* Spatial metagenomic characterization of microbial biogeography in the gut.
467 *Nat Biotechnol* **37**, 877–883 (2019).

468 9. Tyler, A. D. *et al.* Microbiome Heterogeneity Characterizing Intestinal Tissue and Inflammatory
469 Bowel Disease Phenotype. *Inflamm Bowel Dis* **22**, 807–16 (2016).

470 10. Mimee, M., Tucker, A. C., Voigt, C. A. & Lu, T. K. Programming a Human Commensal
471 Bacterium, Bacteroides thetaiotaomicron, to Sense and Respond to Stimuli in the Murine Gut
472 Microbiota. *Cell Syst* **1**, 62–71 (2015).

473 11. Kotula, J. W. *et al.* Programmable bacteria detect and record an environmental signal in the
474 mammalian gut. *P Natl Acad Sci Usa* **111**, 4838–43 (2014).

475 12. Lim, B., Zimmermann, M., Barry, N. A. & Goodman, A. L. Engineered Regulatory Systems
476 Modulate Gene Expression of Human Commensals in the Gut. *Cell* **169**, 547-558.e15 (2017).

13. Olson, E. J. & Tabor, J. J. Optogenetic characterization methods overcome key challenges in synthetic and systems biology. *Nat Chem Biol* **10**, 502–11 (2014).

14. Tabor, J. J., Levskaya, A. & Voigt, C. A. Multichromatic control of gene expression in Escherichia coli. *J Mol Biol* **405**, 315–24 (2010).

15. Schmidl, S. R., Sheth, R. U., Wu, A. & Tabor, J. J. Refactoring and Optimization of Light-SwitchableEscherichia coliTwo-Component Systems. *Acs Synth Biol* **3**, 820–831 (2014).

16. Olson, E. J., Hartsough, L. A., Landry, B. P., Shroff, R. & Tabor, J. J. Characterizing bacterial gene circuit dynamics with optically programmed gene expression signals. *Nat Methods* **11**, 449–55 (2014).

17. Olson, E. J., Tzouanas, C. N. & Tabor, J. J. A photoconversion model for full spectral programming and multiplexing of optogenetic systems. *Mol Syst Biol* **13**, 926 (2017).

18. Milias-Argeitis, A., Rullan, M., Aoki, S. K., Buchmann, P. & Khammash, M. Automated optogenetic feedback control for precise and robust regulation of gene expression and cell growth. *Nat Commun* **7**, 12546 (2016).

19. Chait, R., Ruess, J., Bergmiller, T., Tkačik, G. & Guet, C. C. Shaping bacterial population behavior through computer-interfaced control of individual cells. *Nat Commun* **8**, 1535 (2017).

20. Han, B., Lin, C. J., Hu, G. & Wang, M. C. 'Inside Out'– a dialogue between mitochondria and bacteria. *Febs J* **286**, 630–641 (2018).

21. Clark, L. C. & Hodgkin, J. Commensals, probiotics and pathogens in the C aenorhabditis elegans model. *Cell Microbiol* **16**, 27–38 (2013).

497 22. Han, B. *et al.* Microbial Genetic Composition Tunes Host Longevity. *Cell* **169**, 1249-1262.e13
498 (2017).

499 23. Pédelacq, J.-D., Cabantous, S., Tran, T., Terwilliger, T. C. & Waldo, G. S. Engineering and
500 characterization of a superfolder green fluorescent protein. *Nat Biotechnol* **24**, 79–88 (2005).

501 24. Shaner, N. C. *et al.* Improved monomeric red, orange and yellow fluorescent proteins derived
502 from Discosoma sp. red fluorescent protein. *Nat Biotechnol* **22**, 1567–1572 (2004).

503 25. Torres-Cabassa, A. S. & Gottesman, S. Capsule synthesis in Escherichia coli K-12 is regulated
504 by proteolysis. *J Bacteriol* **169**, 981–989 (1987).

505 26. Sebastián, D., Palacín, M. & Zorzano, A. Mitochondrial Dynamics: Coupling Mitochondrial
506 Fitness with Healthy Aging. *Trends Mol Med* **23**, 201–215 (2017).

507 27. Cho, D.-H. *et al.* S-nitrosylation of Drp1 mediates beta-amyloid-related mitochondrial fission
508 and neuronal injury. *Sci New York N Y* **324**, 102–5 (2009).

509 28. Exner, N. *et al.* Loss-of-Function of Human PINK1 Results in Mitochondrial Pathology and
510 Can Be Rescued by Parkin. *J Neurosci* **27**, 12413–12418 (2007).

511 29. Donato, V. *et al.* Bacillus subtilis biofilm extends Caenorhabditis elegans longevity through
512 downregulation of the insulin-like signalling pathway. *Nat Commun* **8**, 14332 (2017).

513 30. Castillo-Hair, S. M., Baerman, E. A., Fujita, M., Igoshin, O. A. & Tabor, J. J. Optogenetic
514 control of Bacillus subtilis gene expression. *Nat Commun* **10**, 3099 (2019).

515 31. Fernandez-Rodriguez, J., Moser, F., Song, M. & Voigt, C. A. Engineering RGB color vision
516 into Escherichia coli. *Nat Chem Biol* **13**, 706–708 (2017).

517 32. Gautier, A. *et al.* How to control proteins with light in living systems. *Nat Chem Biol* **10**, 533–
518 541 (2014).

519 33. Leopold, A. V., Chernov, K. G. & Verkhusha, V. V. Optogenetically controlled protein kinases
520 for regulation of cellular signaling. *Chem Soc Rev* **47**, 2454–2484 (2018).

521 34. Goglia, A. G. & Toettcher, J. E. A bright future: optogenetics to dissect the spatiotemporal
522 control of cell behavior. *Curr Opin Chem Biol* **48**, 106–113 (2018).

523 35. Deisseroth, K. Optogenetics: 10 years of microbial opsins in neuroscience. *Nat Neurosci* **18**,
524 1213–25 (2015).

525 36. Zhang, F. *et al.* Caenorhabditis elegans as a Model for Microbiome Research. *Front Microbiol*
526 **8**, 485 (2017).

527 37. Couillault, C. & Ewbank, J. J. Diverse Bacteria Are Pathogens of Caenorhabditis elegans.
528 *Infect Immun* **70**, 4705–4707 (2002).

529 38. Ong, N. T. X., Olson, E. J. & Tabor, J. J. Engineering an E. coli near-infrared light sensor. *Acs*
530 *Synth Biol* **7**, 240–248 (2017).

531 39. Ryu, M.-H. & Gomelsky, M. Near-infrared light responsive synthetic c-di-GMP module for
532 optogenetic applications. *Acs Synth Biol* **3**, 802–10 (2014).

533 40. Engler, C., Gruetzner, R., Kandzia, R. & Marillonnet, S. Golden gate shuffling: a one-pot DNA
534 shuffling method based on type IIs restriction enzymes. *Plos One* **4**, e5553 (2009).

535 41. Chen, Y.-J. *et al.* Characterization of 582 natural and synthetic terminators and quantification
536 of their design constraints. *Nat Methods* **10**, 659–664 (2013).

537 42. Baba, T. *et al.* Construction of Escherichia coli K-12 in-frame, single-gene knockout mutants:
538 the Keio collection. *Mol Syst Biol* **2**, 2006.0008 (2006).

539 43. Gerhardt, K. P. *et al.* An open-hardware platform for optogenetics and photobiology. *Sci Rep-*
540 *uk* **6**, 35363 (2016).

541 44. DISCHE, Z. & SHETTLES, L. B. A specific color reaction of methylpentoses and a
542 spectrophotometric micromethod for their determination. *J Biological Chem* **175**, 595–603 (1948).

543 45. DISCHE, Z. A new specific color reaction of hexuronic acids. *J Biological Chem* **167**, 189–98
544 (1947).

545 46. Portal-Celhay, C., Bradley, E. R. & Blaser, M. J. Control of intestinal bacterial proliferation in
546 regulation of lifespan in Caenorhabditis elegans. *Bmc Microbiol* **12**, 49 (2012).

547 47. Castillo-Hair, S. M. *et al.* FlowCal: A User-Friendly, Open Source Software Tool for
548 Automatically Converting Flow Cytometry Data from Arbitrary to Calibrated Units. *Acs Synth*
549 *Biol* **5**, 774–80 (2016).

550 48. Wang, M. C., Oakley, H. D., Carr, C. E., Sowa, J. N. & Ruvkun, G. Gene pathways that delay
551 Caenorhabditis elegans reproductive senescence. *Plos Genet* **10**, e1004752 (2014).

552

553